Effect of Film thickness on Optical and Structural Properties of CdS Thin Films prepared by spray pyrolysis

Mehdi H. Diwan
Department of Physics - College of Science – University of Diyala

Abstract

Cadmium sulphide (CdS) thin films were prepared by the chemical Spray Pyrolysis technique on glass substrates at 400°C. The analysis of x-ray diffraction spectra XRD , patterns indicated the presence of single-phase hexagonal CdS which confirmed through the atomic force micrographs (AFM) images. The structural parameters such as interplannar distance (d), lattice constant (a), grain size (D), and micro strain have been evaluated, The crystal growth became stronger and more oriented as seen in the x-ray diffraction spectra and grain size became larger with increasing in the thickness. The optical properties have been studied in the range (300-900)nm. It is observed that the direct band gap energy is inversely depended on film thickness from (2.36–2.34) eV.

Keyword: CdS thin films, Optical and Structural Properties ,Spray Pyrolysis.

تأثير السمك على الخصائص التركيبية والبصرية لأغشية Cds الرقيقة المحضرة بطريقة التحلل الكيميائي الحراري

مهدي حاتم ديوان
قسم الفيزياء- كلية العلوم –جامعة ديالى

Effect of Film thickness on Optical and Structural Properties of CdS Thin Films prepared by spray pyrolysis

Mehdi H. Diwan

الخلاصة

حضرت أغشية كبريتيد الكادميوم بطريقة التحلل الكيميائي الحراري على قواعد زجاجية وبدرجة حرارة 400 °C أوضحت نتائج فحوصات حيود الأشعة السينية إن الأغشية المحضرة ذات تركيب متعدد التبلور ونوعها أحادي الطور. السداسي وتم تأكيد ذلك من خلال صور مجهر القوة الذرية المتغيرات التركيبية مثل المسافة بين السطوح البلورية (d), ثابت الشبيكة (a), حجم الحبيبات (D) تم دراستها. وأظهرت نتائج فحوصات حيود الأشعة السينية إن حجم الحبيبات يصبح اكبر بزيادة سمك الأغشية , الخصائص البصرية درست في مدى nm(300-900) وأوضحت إن فجوة الطاقة المباشرة المسموحة تتناسب عكسيا مع زيادة سمك الأغشية eV (2.34–2.36) .

كلمات مفتاحية:- تحلل كيميائي حراري , خصائص تجربة , كبريتيد الكادميوم cds .

Introduction

CdS thin films are regarded as one of the most promising materials for heterojunction thin film solar cells. Wide band CdS (Eg = 2.4 eV) has been used as the window material together with several semiconductors such as CdTe , Cu_2S , InP and CuInSe2 with (14–16)% efficiency [1-5]. However due to the high cost of such a material, studies were developed towards polycrystalline compound semiconductors and particularly thin polycrystalline films. The deposition of CdS films has been explored by deferent techniques: thermal evaporation [6, 7], chemical bath deposition (CBD) [8], molecular beam epitaxy (MBE) [9], and spray pyrolysis [10]. Spray pyrolysis though is expensive, requires the use of sophisticated materials and overall, is not very impressive, now gives good quality semiconductors which allows fabrication of solar cells with satisfactory efficiency.

The aim of this work is to produce CdS thin films by spray pyrolysis technique and to investigate their structural, and optical properties. The effects of film thickness on the structural and optical properties of CdS thin films where many parameters investigated through the structural and optical analysis.

Experimental details

The spray pyrolysis technique is a simple technology in which an ionic solution–containing the constituent elements of a compound in the form of soluble salts–is sprayed onto over heated substrates using a stream of clean, dry air , The apparatus we used for our sprayed process is diagrammed in Figure (1) , and has been described in references [11, 12]. The CdS thin films were prepared by spraying an aqueous solution (0.1)M of cadmium chloride ($CdCl_2$) and 0.1 M thiourea [$(NH_2)_2CS$] on glass substrate kept at (400 ◦ C). The atomization of the chemical solution into a spray of fine droplets was effected by the spray nozzle, with the help of compressed air as carrier gas. The spray rate was about (15 cm^3 /min) through the nozzle ensures a uniform film thickness. The substrates were commercial glass slides with (1mm) thick and (2.5 ∗ 7.5) cm^2 size. Before the spraying substrates were cleaned by detergent solution then washed by deionised water and finally they were cleaned by using ethanol solution. and are placed on afitted socket on the surface of the substrate heater when sprayed. The heater is a cylindrical stainless steelblock furnace electrically controlled to an accuracy with (± 2 ◦ C). The substrate temperature was varied, while the other spray parameters were kept constant. The film thickness was measured by weighting method through using sensitive balance , spraying the solution had been done many times to obtain the required thickness.

The X-ray diffraction (XRD) analysis of the films were recorded with a SHIMADZU 6000X-ray diffractometer operating at (λ=1.541874 A°) by using Cu kα source radiation at (40 kV) and (30 mA) with angle range (10-80). Atomic Force Microscopy AFM (AA 3000 SPM User"s Manual) was used to study the surface morphology of the film. The force applied by the tip was carefully adjusted to avoid any noticeable tip induced damage during scanning. The AFM topography data were used to calculate the average roughness and grain size. Transmission spectra T and Optical energy gap Eg of the deposited films were measured by normal incidence of light, using a double beam UV-VIS spectrophotometer model Cintra-5-GBC, in the wavelength range (300- 900) nm, using a blank substrate as a reference.

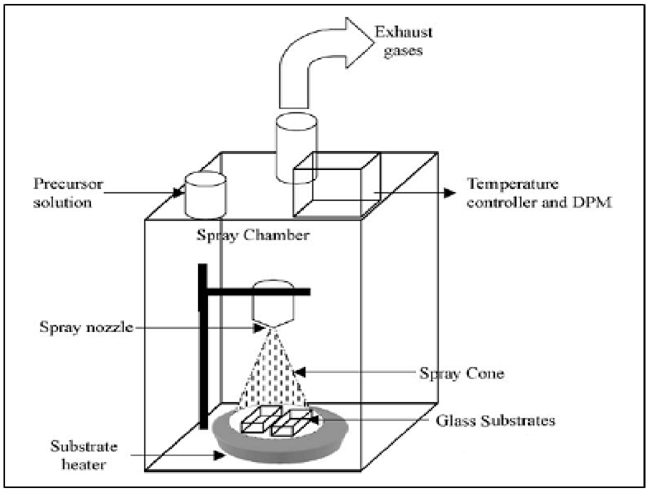

Figure 1. Spray pyrolysis set-up used for thin film preparation.

Results and discussions

1. structure properties

XRD were used to characterize the structural properties of CdS thin films. Diffractograms of CdS films prepared at different thickness (2000 °A and 4000°A) are shown in Figure (1). The X-ray diffraction patterns of the CdS thin films reveald the films are mited of polycrystalline hexagonal (wurtzite) structure. The diffraction single peak existed at (2θ = 26.26°) It is confirmed by comparing the peak positions 2θ of the XRD patterns of the films with the standard X-ray powder diffraction data file (card no. 06-0314). And the corresponds plane is crystallines (002) hexagonal [13, 14].The degree of preferred orientation with the increasing the thickness. No other peaks beside these is observed beside the establishes the single phase hexagonal structure of the films [15].

It was observed that the increase of the thickness increase the diffraction peak intensity of (002) plane which resulted in increase in grain size and good crystallinity of the films and the full width at half maximum (FWHM) decreases from (0.10110^0 to 0.0600^0)and these peaks are shifted to higher diffraction angle from (26.21^0 to 26.23^0)The effect of thickness on the grain size (GS) of the obtained phase was also investigated. If the broadening is due only to the effect of crystallite size, grain size can be simply determined from the (002) diffraction line using the Debye-Scherrer formula [16]:

$$D = \frac{K\lambda}{\beta_{2\theta} COS\theta} \qquad (1)$$

Where β is the full width at half maximum (FWHM) of the peak corrected for instrumental broadening, λ is the wavelength of the X-rays, and K is the Scherrer constant, which generally depends on the crystallite shape. Considering that the Scherrer constant K is equal to unity according to the widespread practice, and that the effect of residual macro strain is negligible. Grain size with the two thicknesses (2000°A to 4000°A) are shown in table (1)

The lattice constant `*a*' for the hexagonal phase structure is determined by the relation [17]:

$$\mathbf{a = d*(h^2+k^2+l^2)^{1/2}} \qquad (2)$$

where'd' is the distance between atomic planes, which is calculated by using bragg law, as it is clear in table(1) 'a' decreases for thicker film. The lattice contraction occurs because of higher surface to volume ratio [18].

Other causes for XRD peaks being broader than expected based on crystal size is the presence of strain in the crystals or other defects, such as dislocations, which destroy the long-range lattice order. The micro strain (□) developed in the CdS film is calculated from the relation [19]:

□= (Bcos□)/4 (3)

The change in lattice constant 'as seen above' for thicker thin film suggests that the film grains are strained and that may be owing to the change of nature and concentration of the native imperfections. As shown in table (1), the micro strain decreases from **(0.001852)** to **(0.00142)** after increasing film's thickness. There is a close correlation between micro strain decreasing and crystallite size increasing , because both phenomena lead to the phase crystallinity changing [20] .Due to the increase in crystalline size with increasing film's thickness, the defects in the lattice is reduced, which in turn, reduces the micro strain.[21].

Table (1). Structural parameters of CdS thin films with 200 and 400 nm thickness.

Orientation	2θ[deg.]		Grain Size (nm)		d (nm)		(a) (nm) calculated		(a) (nm) ASTM
	(200nm)	(400nm)	(200nm)	(400nm)	(200nm)	(400nm)	(200nm)	(400nm)	
[002]	26.2100	26.2385	87.57	135.89	0.34101	0.34064	0.68202	0.68128	0.5818
	Micro strain								
	(200nm)				(400nm)				
	0.00395				0.000255				

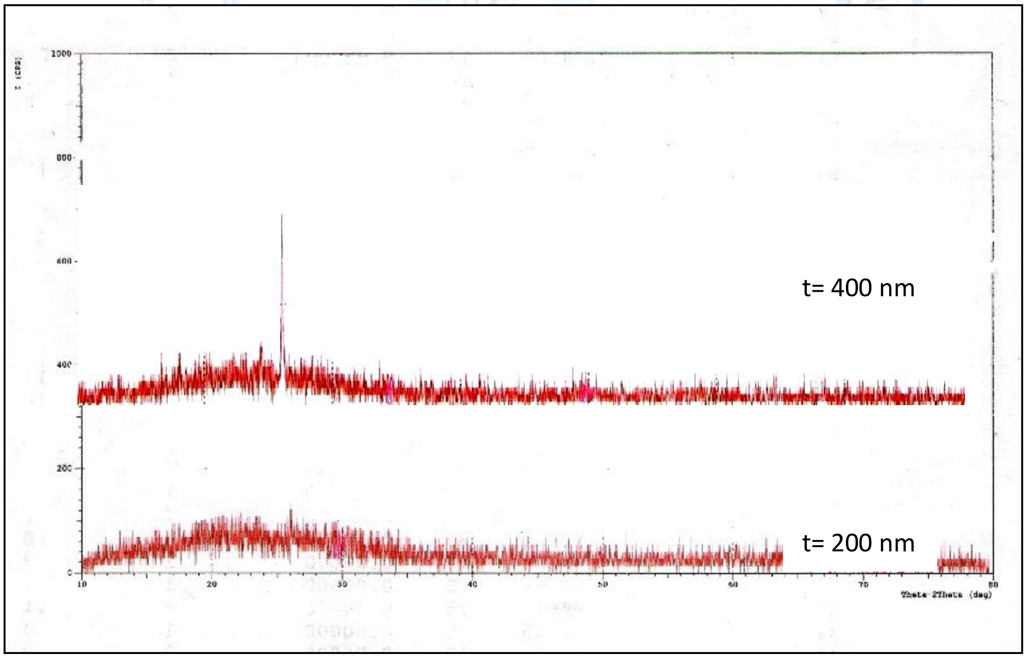

Figure 2. X-Ray diffractograms of CdS films with different thicknesses

2. Surface morphology

In order to investigate the morphology of CdS thin films deposited on glass, atomic force micrographs were recorded for (2 x 2) μm 2 regions. The average size and rms surface roughness measured for the CdS thin films, indicate that surfaces and cross-section of CdS layers, deposited at various substrate temperatures are given in figure 3. All the films show that the particles are closely bonded and no voids are observed.

Fig. 3a & 3b show cluster of particles with highly dense structure. The CdS thin films layer has the advanced surface and typical columnar structure with highly dense grains . Fig. 3a shows typical (2×2μm) AFM images 2-D, 3-D of CdS film deposited on glass at a substrate temperature of (200 nm). It shows a homogeneous formation of film and with no voids observed in the structure. This means that the film is very dense structure with high packing density. The average grain size diameter of the CdS film was (76.9 nm) with an average roughness of 7.91 nm and a root mean square roughness of (10.5 nm).

Fig. 3b shows a typical (2×2μm) AFM images 2-D, 3-D of CdS film deposited on glass at a substrate temperature of (400 nm). The average grain size diameter of the CdS film was (68.6 nm) with an average roughness of (9.79 nm) and a root mean square roughness of (12.6 nm). Observed in Fig. 3a & 3b The increase of thickness further from (200 to 400) nm gives the crystalline increment of the surface relief of CdS layer. In the increase of columnar structures grain size with decrease The average diameter. AFM images also revealed that CdS films become more uniform and dense with the increase of thickness .The average grain size of the film, observed by AFM is smaller than that calculated from XRD pattern. This may well be due to defects such as twins, and dislocations, etc., induced into the crystallites during the growth [22].

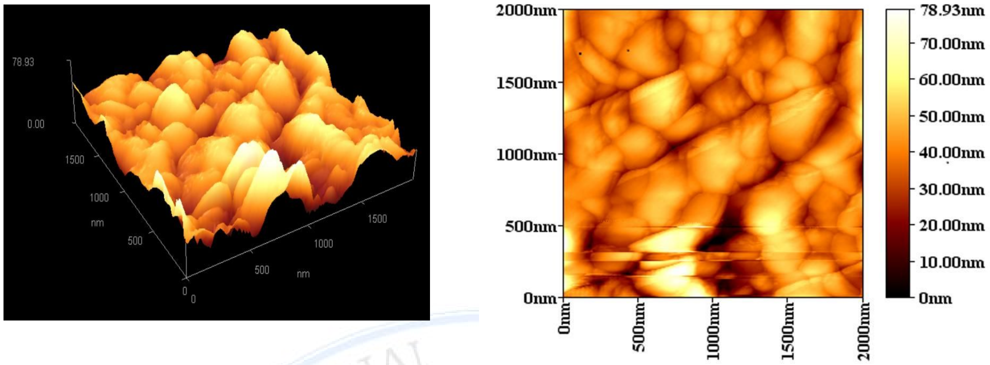

Figure(3a). AFM images morphology of CdS film at the thickness (200 nm).

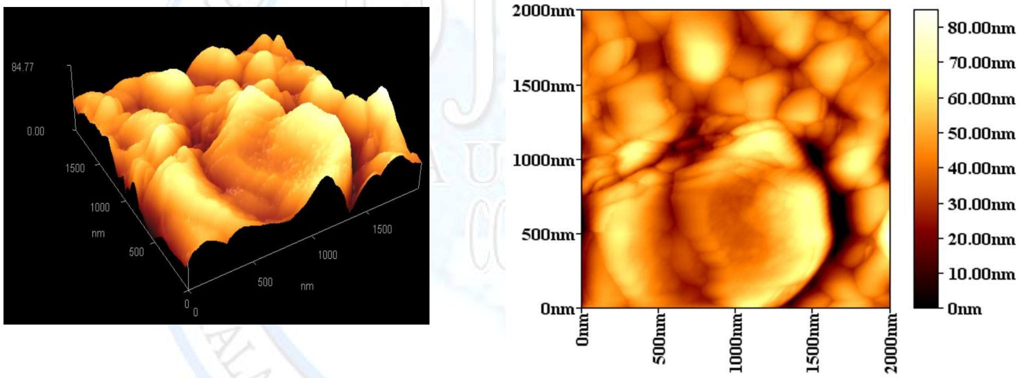

Figure (3b). AFM images morphology of CdS film at the thickness (400 nm).

3. Optical properties

In Fig 7, the variation of optical Reflectance as a function of wavelength in the range of (300-900) nm for the CdS films with different thickness were in the visible region. In general, the Reflectance spectra increase with an increase in the thickness. This improvement result from the improvement in perfection and stoichiometry of the CdS films [23].

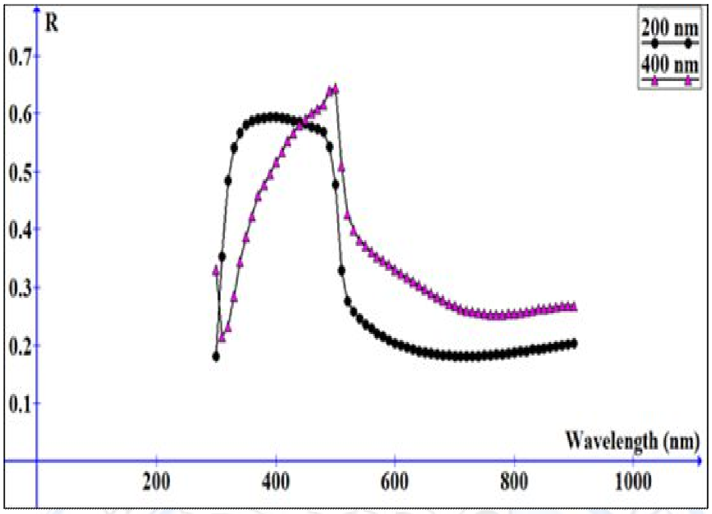

Figure 4. Reflectance Spectra of CdS thin films as a function of wavelength

From the Fig.8 Optical properties of CdS thin films are determined from absorbance measurements in the range of (300-900)nm. The absorption coefficient can be written in terms of the incident radiation energy.

$\alpha = A\,(h\gamma - Eg)$ (4)

Where 'h' is the Planck's constant and 'γ' is the frequency of the incident radiation. Absorption coefficient (α) associated with the strong absorption region of the films was calculated from absorbance (A) and the film thickness (t) using the relation.

$A = 2.3026\ A/t$ (5)

The absorption coefficient of these films at different thicknesses. A close examination of Fig. 8 reveals that the thick film have lower α value at high energy region than the thin film. The absorption coefficient shows oscillatory behavior at the forbidden gap region. It is also observed that the thinner film have high α value in the band-to band absorption region. This effect may be explained by proposing that thicker film have bigger crystallites (grains), so they are closer to bulk crystalline CdS, but bigger grain sizes results in larger unfilled inter-granular volume so the absorption per unit thickness is reduced [24].

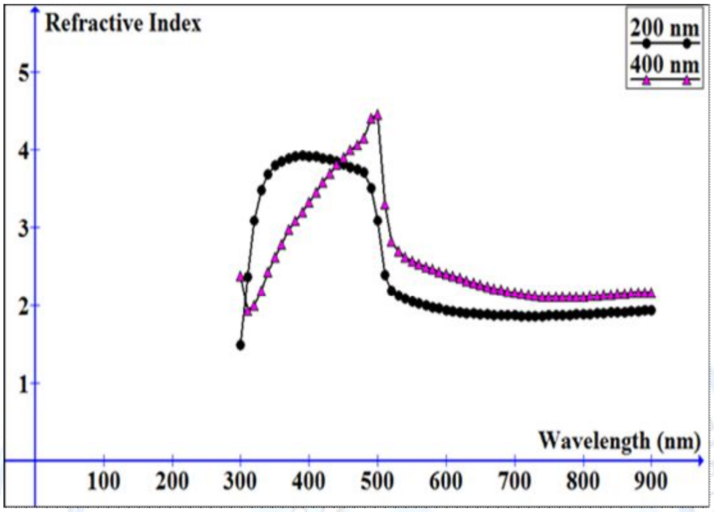

Figure 5. Refractive index Spectra of CdS thin films as a function of photon energy

The Extinction coefficients are calculated using the equation.

$K_\circ = 2.303\ \lambda \log(1/T0) / 4\pi d$ (6)

From the Fig. 9. The value of Extinction Coefficient ($K_\circ$) decreases with the increases in the film thickness. The extinction coefficient $K_\circ$) is directly related to the absorption of light. In the case of polycrystalline films, extra absorption of light occurs at the grain boundaries [25]. This leads to non-zero value of ($K_\circ$) for photon energies smaller than the fundamental absorption edge [26].

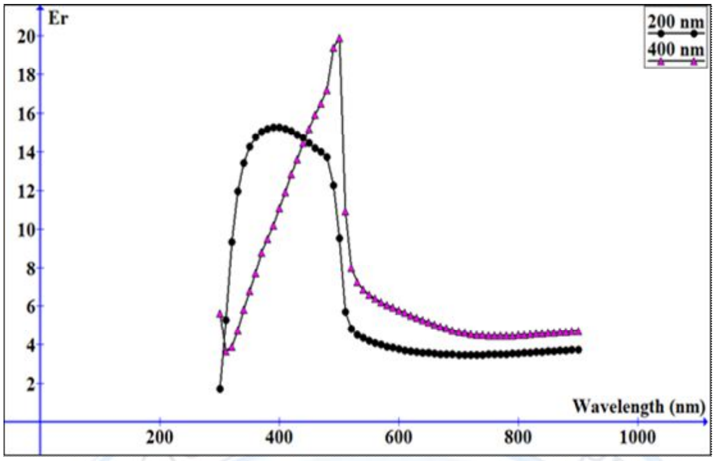

Figure 6. Real part of dielectric constant(E_r) of CdS thin films as a functions of wavelength

The optical band gab can be obtained by extra plotting the linear portion of the plot $(\alpha h\gamma)^2$ versus hγ. From the plot, the variation of $(\alpha h\gamma)^2$ Versus photon energy for the two thicknesses (2000 Å, 4000 Å) CdS thin films are shown in Fig. 12. The observed decrease in the band gap energy with increases in thickness is due to the changes in the barrier height to the size of the grain in crystalline film and large density of dislocation.

The presence of a single slope in the curves suggests that from Chemical spray pyrolysis are of single phase in nature and the type of transition is direct and allowed [27]. From these absorption peaks, the direct and allowed band gap energy is evaluated from the plot $(\alpha h\gamma)^2$ Versus hγ are shown in table (3).

Table (3). Variation of energy gap with thickness

Band gap energy (eV)	Thickness Å
2.36	2000
2.34	4000

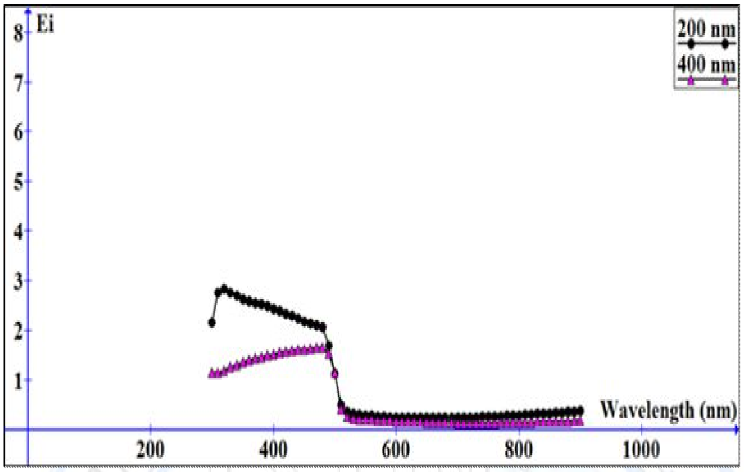

Figure 7. Imajinary part of dielectric constant of CdS thinfilms as a function of photon energy

Conclusion

Structural and optical properties of CdS films were sensitive to the thickness .It was found that the The crystallinity of films increased with the increase of thickness, where the grain size becomes larger and it denser. The films became more uniform and dense with the increase of thickness. Optical measurements, showed an increasing optical transmission with increasing thickness. The energy band gap was sensitive to the variation of thickness and decrease with increase the thickness and the films exhibited a direct transition in the range (2.36 - 2.34) eV dependening on the thickness.

References

1. K.D. Dobson, I. Visoly-Fisher, G. Hodes and D. Cahen, Solar Energy Materials & Solar Cells, 62, 295(2000).
2. S.R. Das, P. Nath, A. Banerjee and K.I. Chopra, Solid State Commun, 21,49(1977).
3. L.M. Frass and Y. Ma, J. Cryst. Growth,39, 92(1977).
4. J.R. Tuttle, J.S. Ward and A. Dudn, Proc.1996 Spring MRS Meet,San Francisco,CA486, p.143(1996).
5. B. Su and K.L. Choy, Thin Solid Films, 359,160(2000).
6. A. Ashour, N. El-Kadry and S.A. Mahmoud, Thin Solid Films, 269,117(1995).
7. S.A. Mahmoud, A.A. Ibrahim and A.S. Riad, Thin Solid Films, 372,144(2000).
8. A.I. Oliva, O. Solis-Canto, R. Castro-Rodriguez and P. Quintana, Thin Solid Films,391,28(2001).
9. Ph. Ho_majnn, K. Horn, A.M. Bradshaw, R.L. Johnson, D. Fuchs and M.Cardona, Phys. Rev., B47,1639,(1993).
10. I.K. Battisha, H.H. A_fy, G. Abd El-Fattah and Y. Badr, Fizika,A11,31(2002).
11. A. Ashour, H.H. A_fy and S.A. Mahmoud,Thin Solid Films, 248,253(1994).
12. B. Thangaraju, Thin Solid Films, 402,71(2002).
13. L.J. Van der Pauw, Philips Res. Rep., 13,1(1958).
14. A.A. Ramadan, R.D. Gould and A. Ashour, Thin Solid Films, 239,272(1994).
15. thesis, ABDULLAH SERHAN AL-SHAMMARI, King Saud University College of Science,(2005).
16. G. Laukaitis, S. Lindroos, S. Tamulevi_cius and M. LeskelTM, Applied Surface Science,185, 134(2001).
17. Chalcogenide Letters Vol. 5, No.11,p. 265 – 271, November (2008).
18. K. K.Nanda, S, N. Sarangi,S. N. Sahu Nano Structured Material 10,1401(1998).
19. Kr Kalita P. , Ksarma B. , Das H. L. , J.Bull. Mater. Sci.,Vol. 23, No. 4,pp. 313–317 August (2000).
20. Thin Solid Films 517 976–981,(2008).
21. Journal of New Materials for Electrochemical Systems 10,9-14(2007)

22. Ning Xu, Yingliang Xu, Li Li, Yiqun Shen, Tinwei Zhang, Jiada Wu, Jian Sun and Zhifeng Ying, J. Vac. Sci. Technol. A, 24,517(2006).
23. A. Ashour, H.H. A_fy and S.A. Mahmoud, Thin Solid Films, 248,253(1994).
24. J. Lee, Thin Solid Films 451-452,170(2004).
25. V. Damodara Das, K.Seetharama Bhat, J. Material Science-Materials in Electronics 1**,**169 (1990).
26. T. Mahalingam, M.Radhakrishnan, C.Balasubramaniam, Thin Solid Films 78 (3) 299(1981).
27. H.Metin, R.Esen, Semicond.Sci.Technol,18**,**647(2003).